Electronic Supplementary Material (ESI) for Journal of Materials Chemistry A.

Nano-spatially confined and interface-controlled lithiation-delithiation combined in in-situ formed (SnS-SnS_2-S)/FLG composite: A route to ultrafast and cycle-stable anode for lithium-ion batteries

Deliang Cheng[a], Lichun Yang[a], Jiangwen Liu[a], Renzong Hu[a], Jun Liu[a], Ke Pei[b], Min Zhu[a] and Renchao Che*[b]*

[a]Guangdong Provincial Key Laboratory of Advanced Energy Storage Materials, School of Materials Science and Engineering, South China University of Technology, Guangzhou 510641, China

* E-mail: memzhu@scut.edu.cn

[b]Laboratory of Advanced Materials, Department of Materials Science and Collaborative Innovation Center of Chemistry for Energy Materials, Fudan University, Shanghai, 200438, China

* E-mail: rcche@fudan.edu.cn

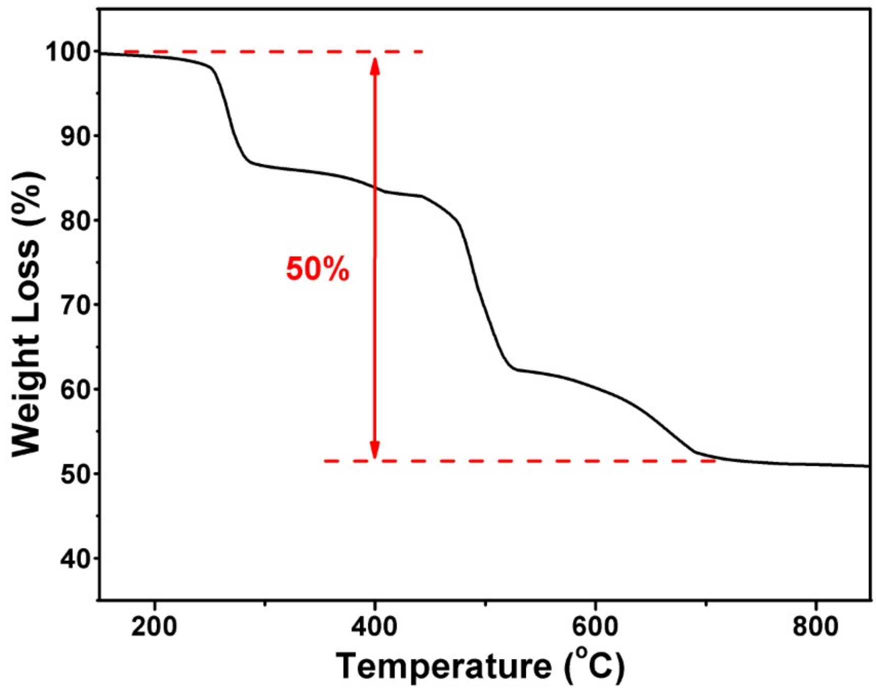

Fig. S1. TG profile of (SnS-SnS_2-S)/FLG.

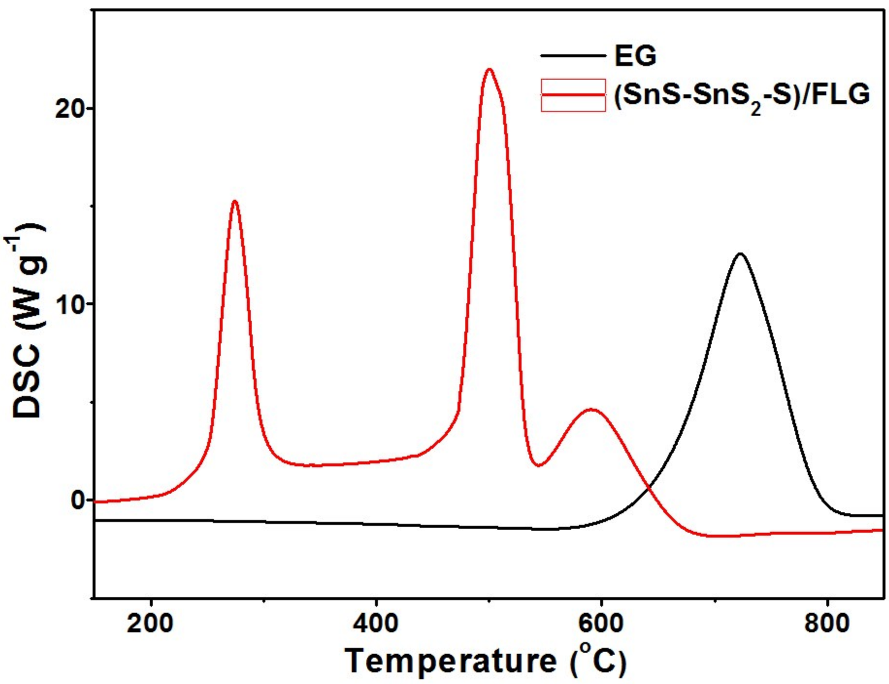

Fig. S2. DSC curves of EG and (SnS-SnS_2-S)/FLG.

Calculation of contents of SnS, SnS_2, S, FLG in the (SnS-SnS_2-S)/FLG composite.

① Based on the deconvoluted peak areas, the ratio of Sn^{4+}/Sn^{2+} is 0.4, the ratio of S^{2-}/S^0 is 1.48. Set the content of SnS is x, so the content of SnS_2 is 183*0.4x/151, the content of S is 32*(x+0.4x*2)/1.5/151, respectively.

② Based on the TG curve of the (SnS-SnS_2-S)/FLG composite, 50 wt% of the weight is lost during 200~800 ^{o}C, which originates from the combustion of S, FLG and oxidation of SnS_x.

$SnS + O_2 \rightarrow SnO_2 + SO_2$		Δm	$SnS_2 + 3O_2 \rightarrow SnO_2 + 2SO_2$		Δm
151	151	0	183	151	32
x	x	0	183*0.4x/151	0.4x	32*0.4x/151

Set the content of FLG is y, and then equations can be:

$$\begin{cases} x + 183*0.4x/151 + 32*1.2x/151 + y = 1. \\ 32*0.4x/151 + 32*1.2x/151 + y = 0.50. \end{cases}$$

So x = 0.357, y = 0.379.

Finally, the contents of SnS, SnS_2, S, FLG in the (SnS-SnS_2-S)/FLG composite can be determined to be 35.7, 17.3, 9.1, 37.9 wt%.

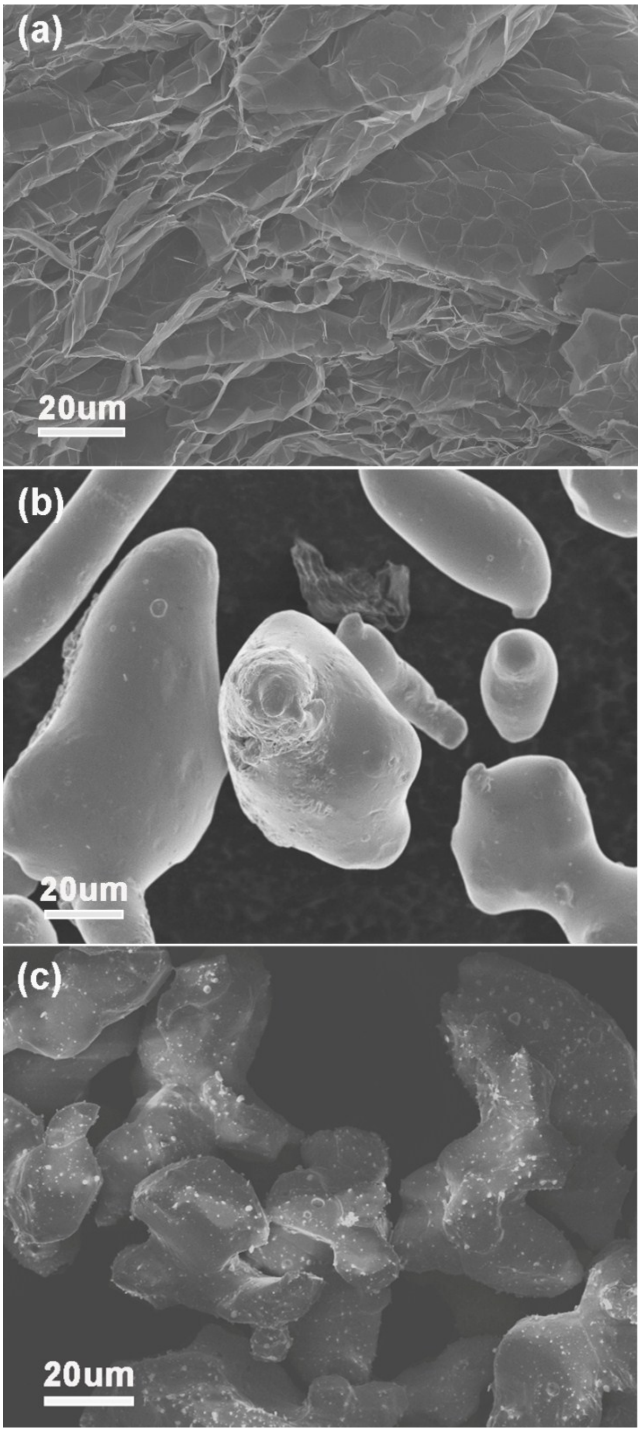

Fig. S3. SEM images of (a) EG powder, (b) Sn powder, (c) S powder.

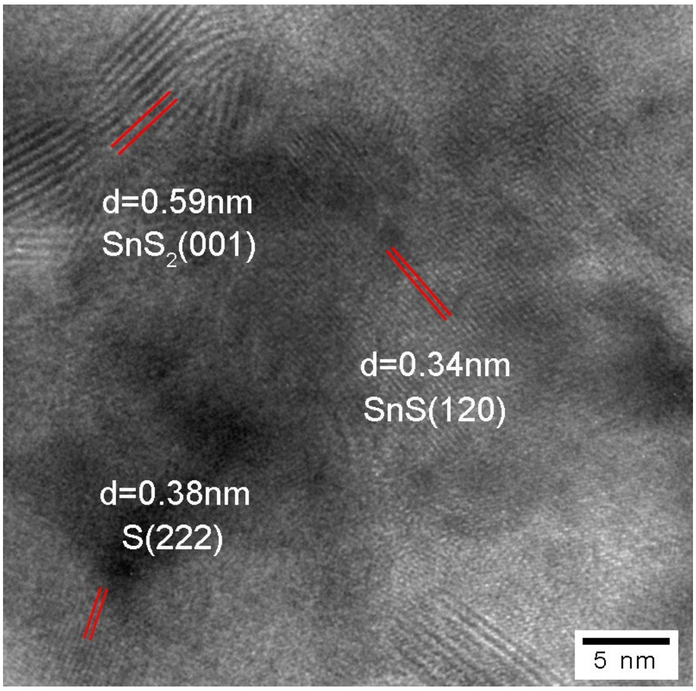

Fig. S4. HRTEM image of the SnS-SnS_2-S.

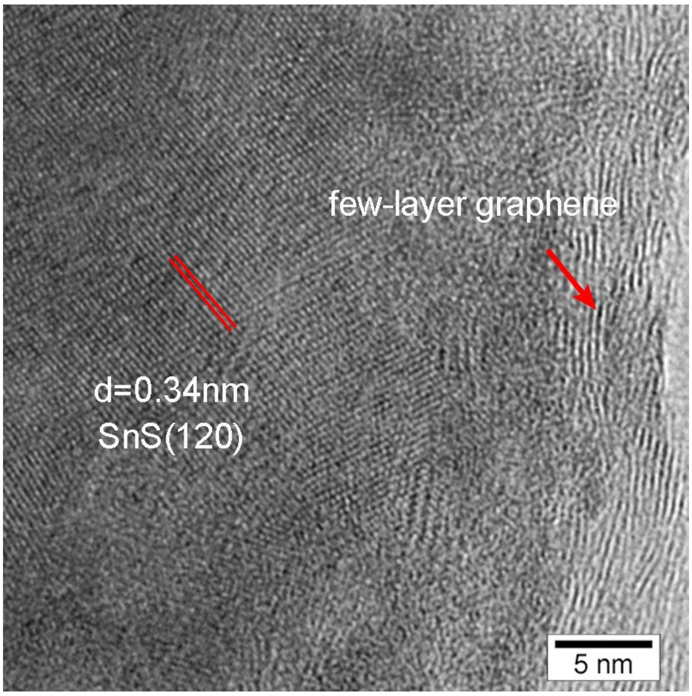

Fig. S5. HRTEM image of the SnS/FLG.

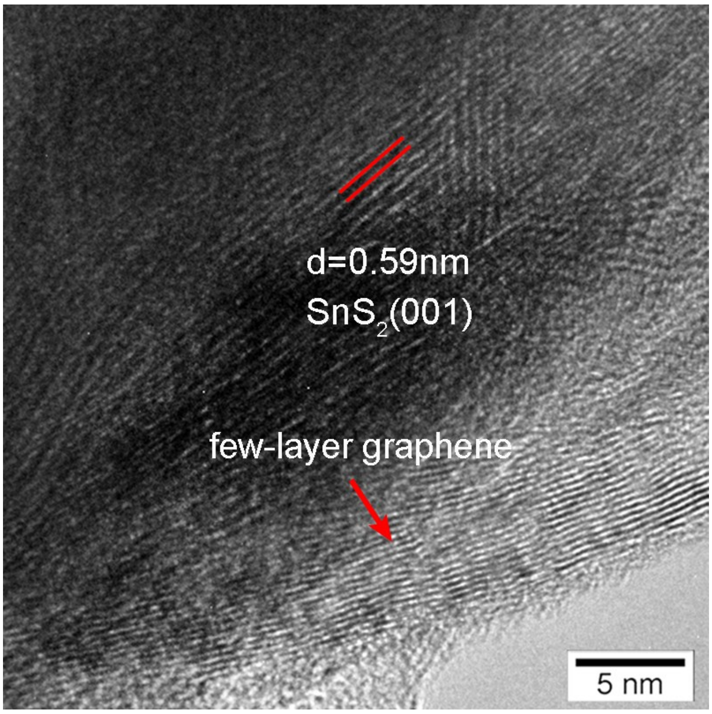

Fig. S6. HRTEM image of the SnS_2/FLG.

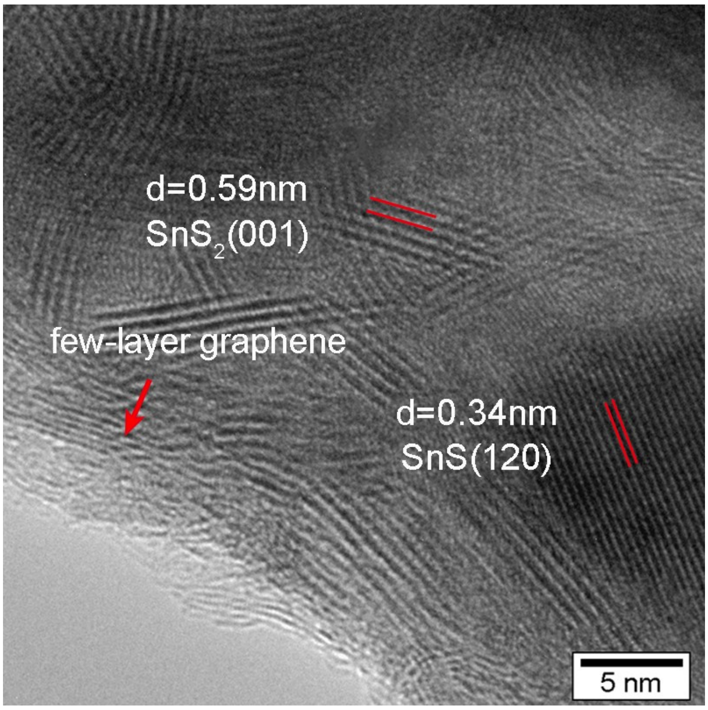

Fig. S7. HRTEM image of the (SnS-SnS_2)/FLG.

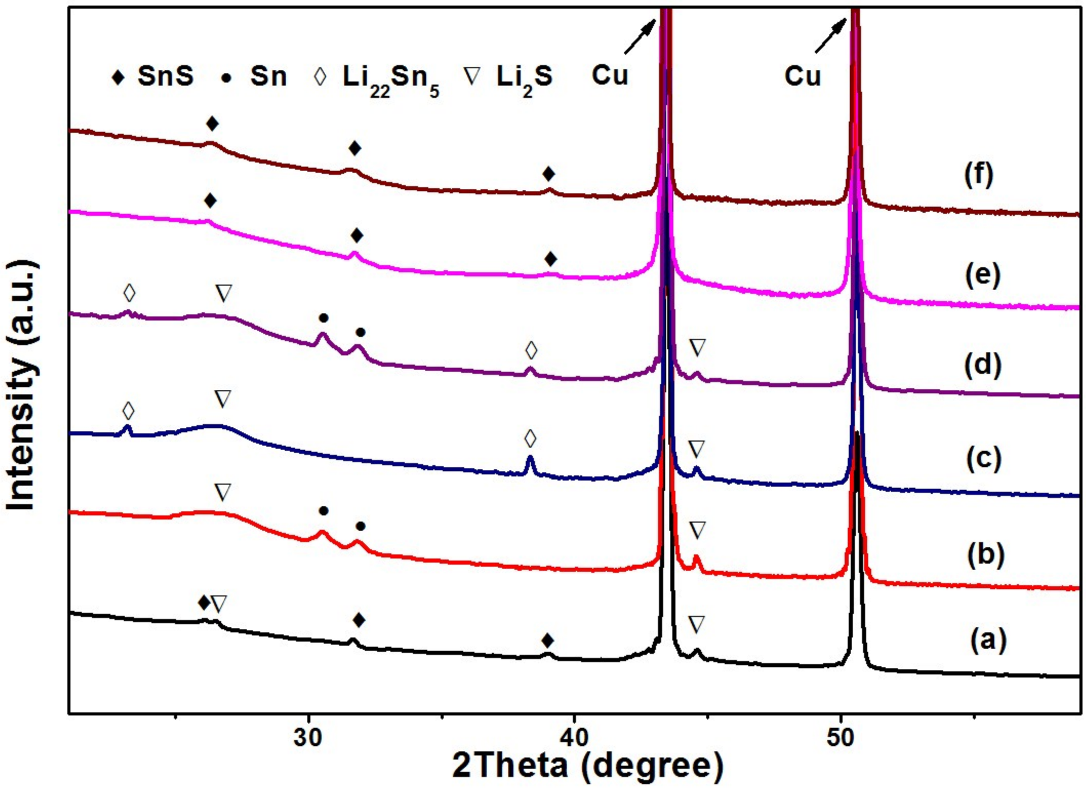

Fig. S8. Ex-situ XRD patterns of the (SnS-SnS_2-S)/FLG anode taken at different discharge/charge states (vs. Li/Li^+): (a) discharged to 1.6 V, (b) discharged to 0.85 V, (c) discharged to 0.01 V, (d) charged to 0.80 V, (e) charged to 2.0 V, (f) charged to 3.0 V. (Discharged/charged galvanostatically at 0.05 A g^{-1}).

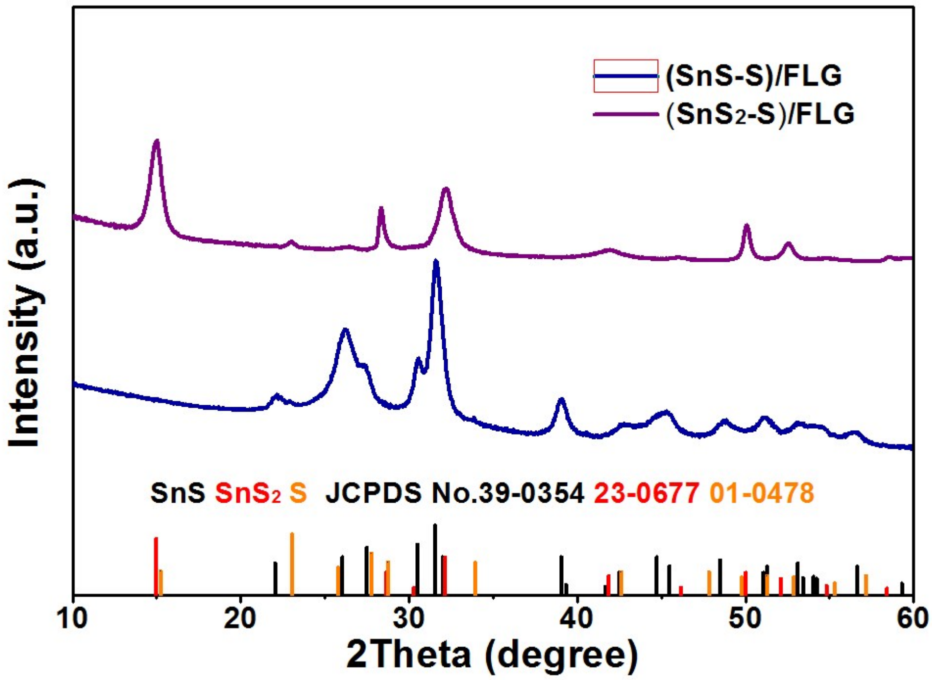

Fig. S9. XRD patterns of the (SnS-S)/FLG and (SnS_2-S)/FLG.

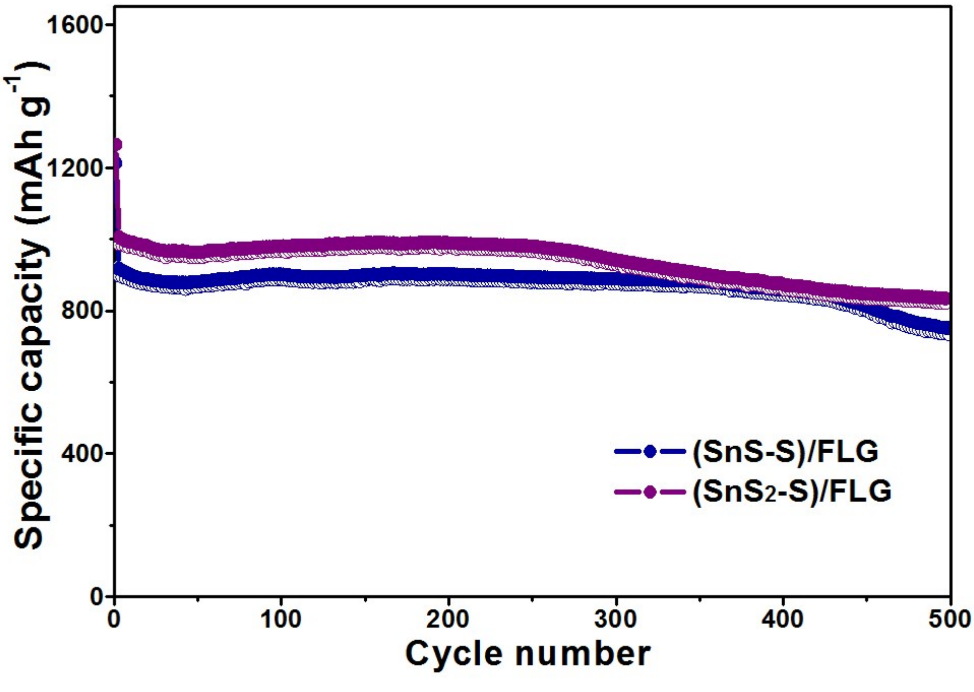

Fig. S10. Cycling performance of the (SnS-S)/FLG and (SnS_2-S)/FLG tested at 0.2 A g^{-1}.

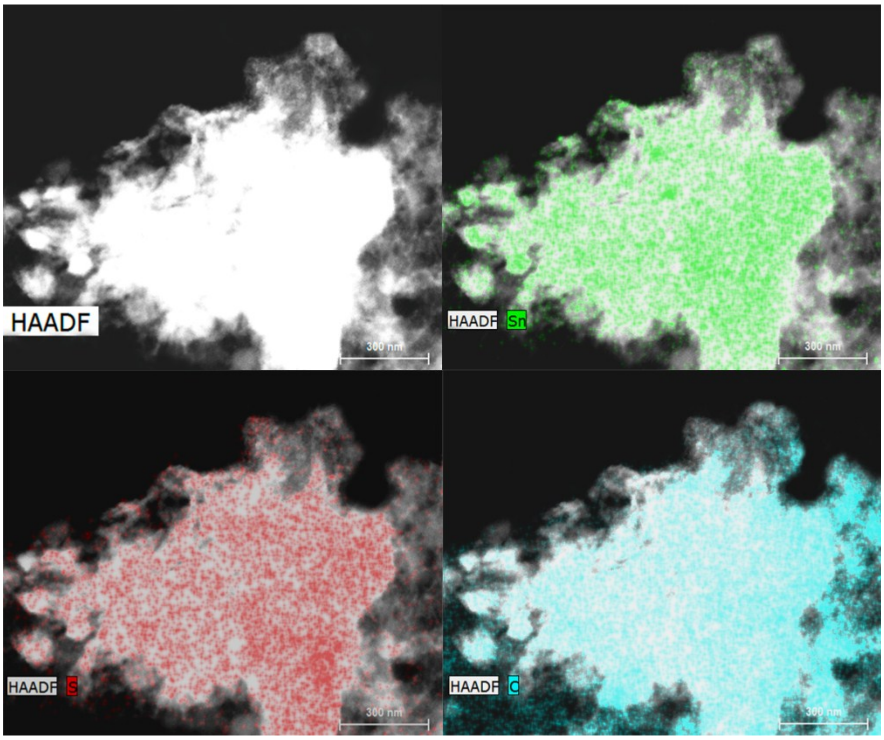

Fig. S11. Elemental mapping of (SnS-SnS_2-S)/FLG after 500 charge/discharge cycles.

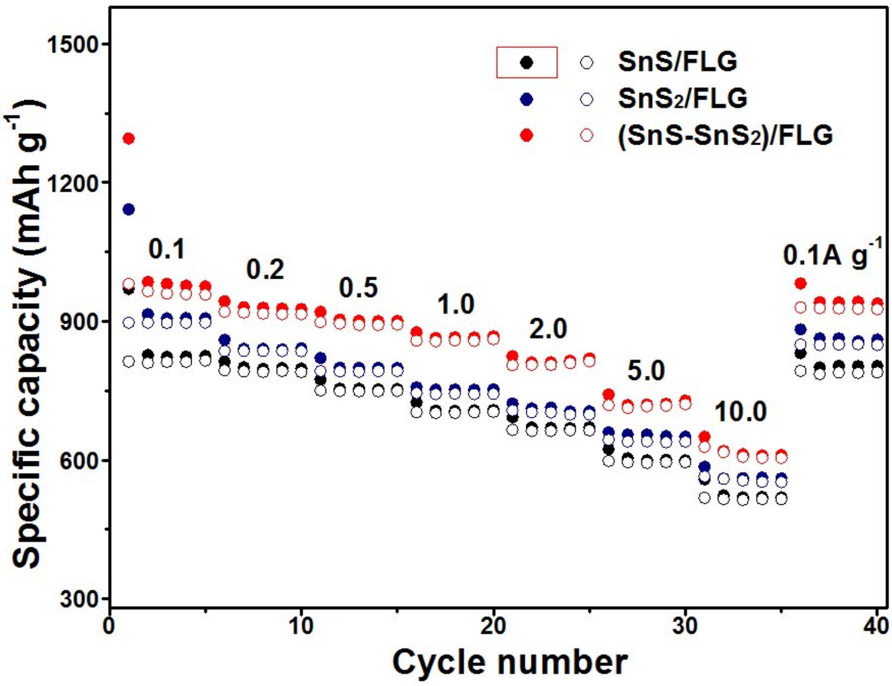

Fig. S12. Rate performance of SnS/FLG, SnS_2/FLG and (SnS-SnS_2)/FLG tested at various current densities (vs. Li/Li^+).

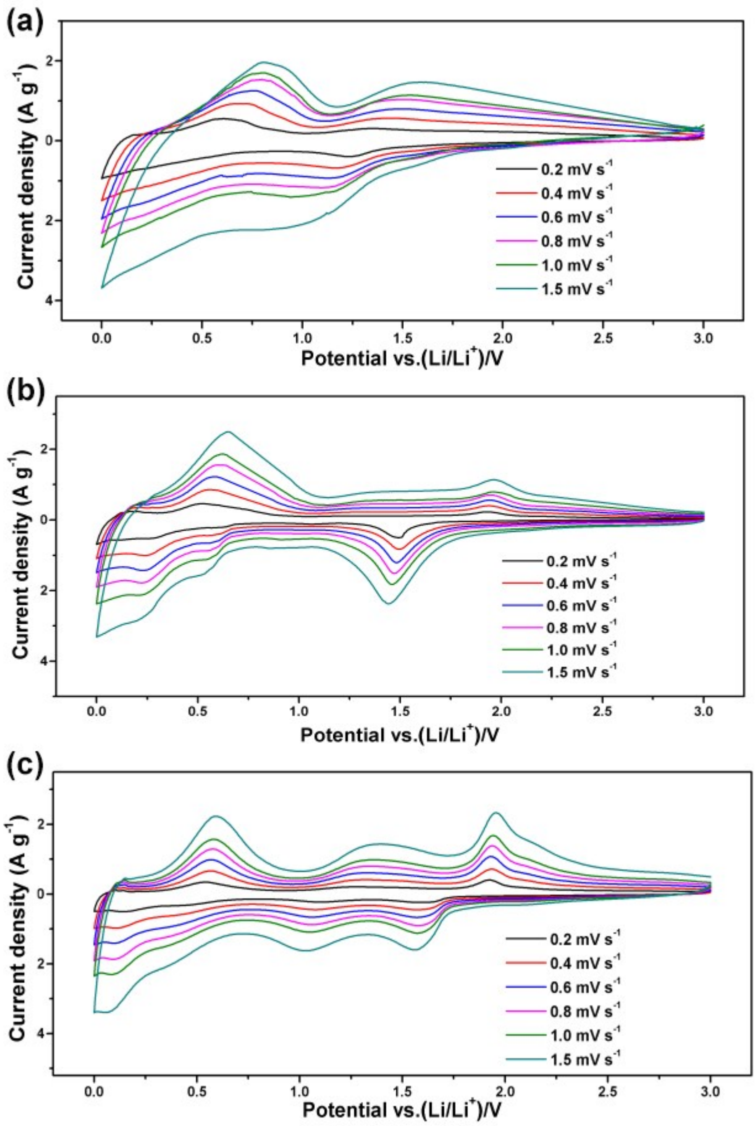

Fig. S13. CV curves of (a) SnS/FLG, (b) SnS_2/FLG and (c) (SnS-SnS_2)/FLG at various scan rates, from 0.2 to 1.5 mV s^{-1}.

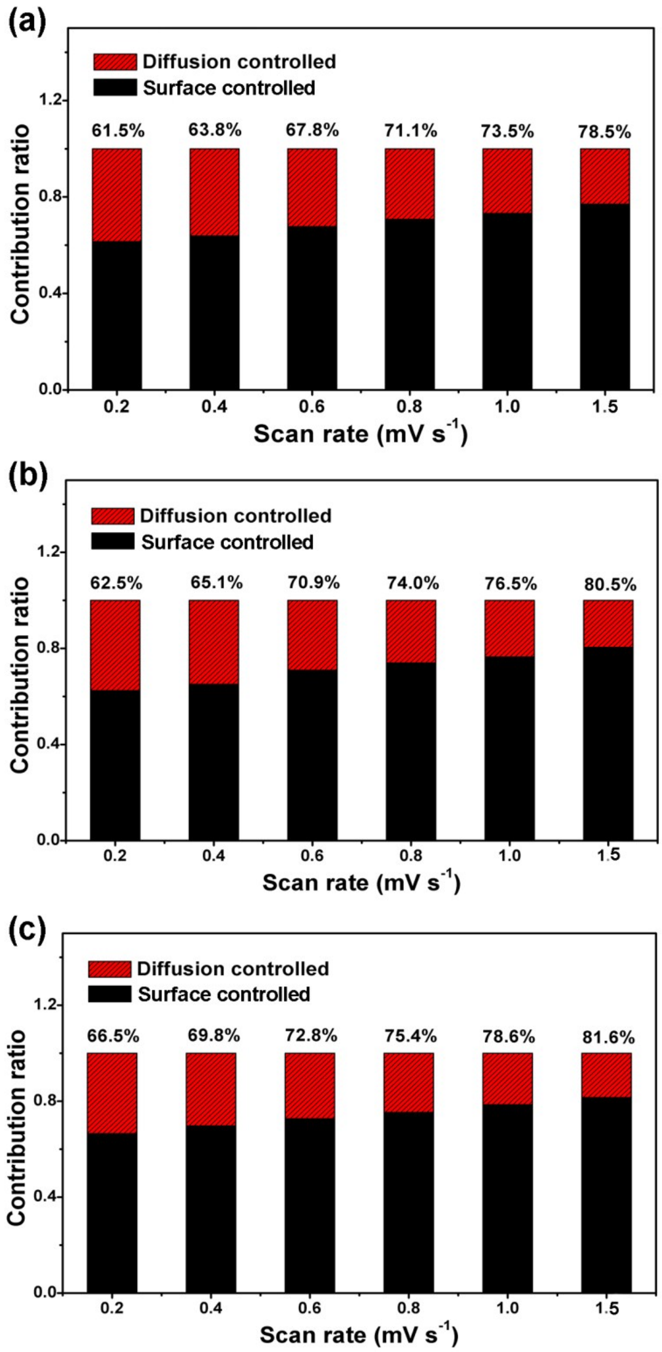

Fig. S14. Capacitive contribution at different scan rates of (a) SnS/FLG, (b) SnS_2/FLG and (c) (SnS-SnS_2)/FLG.

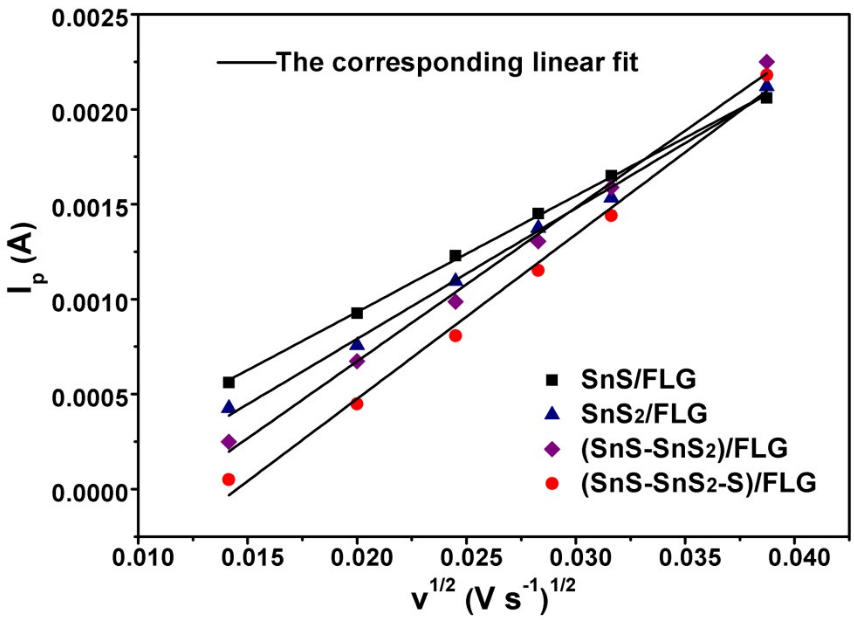

Fig. S15. Corresponding relationship between peak currents and sweep rates of the SnS/FLG, SnS_2/FLG, (SnS-SnS_2)/FLG and (SnS-SnS_2-S)/FLG.

The anodic peak currents I_p at different scan rates are adopted to calculate the Li^+ diffusion coefficients (D) of these electrodes according to the following Randles Sevcik equation: $I_p = 2.69\times10^5ACD^{1/2}n^{3/2}\upsilon^{1/2}$, where A stands for the anode area (cm^2), C is for the shuttle concentration (mol cm^{-3}), n is for the involved electron numbers in the redox action, and υ is for the scan rate (V s^{-1}). With this data, a fitting straight-line can be obtained with $\upsilon^{1/2}$ as the x-axis and I_p as the y-axis. Therefore, the line slope and Li^+ diffusion coefficient can be calculated and listed in Table S1.

Table S1. Line slopes and Li^+ diffusion coefficients of the SnS/FLG, SnS_2/FLG, (SnS-SnS_2)/FLG and (SnS-SnS_2-S)/FLG.

Sample	Line slop	Diffusion coefficient (cm^2 s^{-1})
SnS/FLG	0.06115	3.96×10^{-7}
SnS_2/FLG	0.06791	4.96×10^{-7}
(SnS-SnS_2)/FLG	0.08027	6.83×10^{-7}
(SnS-SnS_2-S)/FLG	0.08695	8.01×10^{-7}

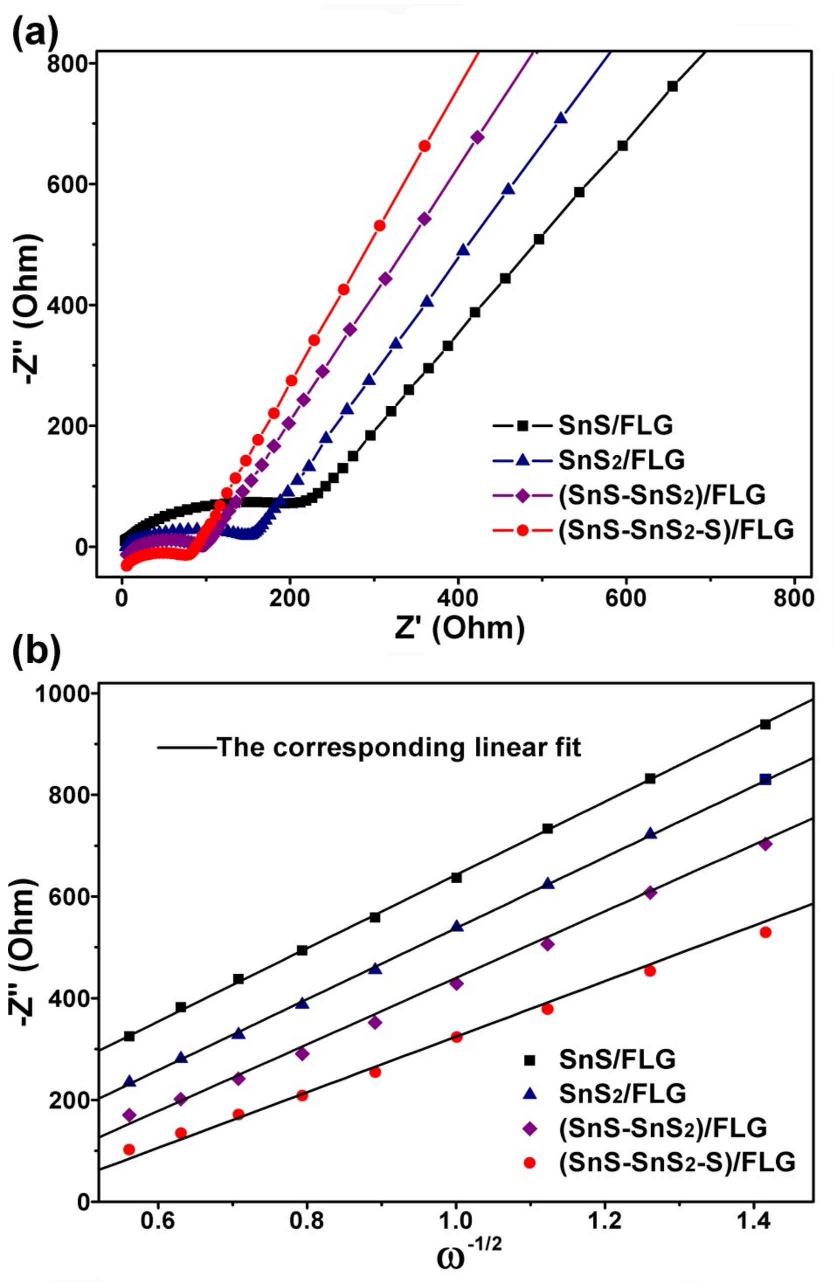

Fig. S16. (a) Nyquist plots, (b) the corresponding linear fits in the low-frenquency region of the SnS/FLG, SnS_2/FLG, (SnS-SnS_2)/FLG and (SnS-SnS_2-S)/FLG.

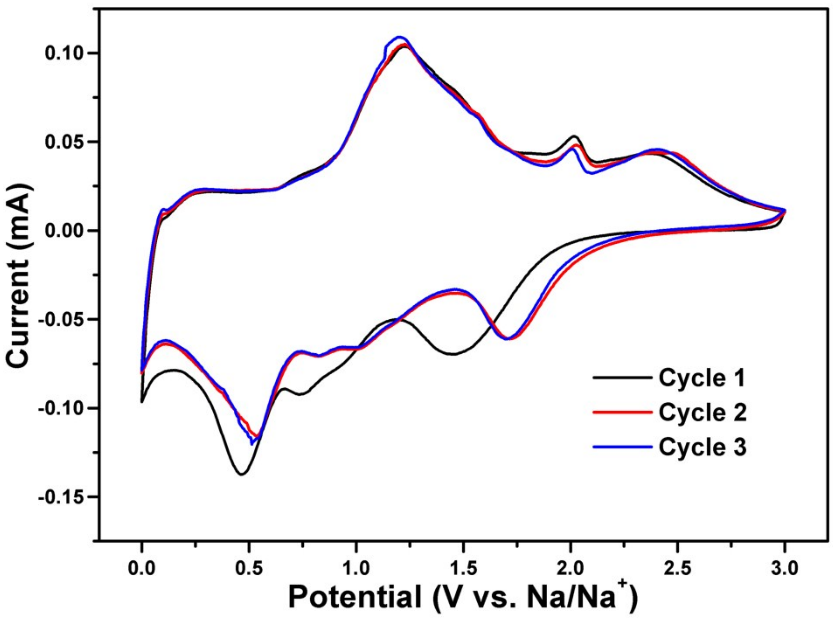

Fig. S17. CV profiles of (SnS-SnS_2-S)/FLG scanned at 0.1 mV s^{-1} (vs. Na/Na^+).

In the first cathodic sweep, the peaks located at 0.75~1.95 V associate with the conversion reaction of S and SnS_x with Na^+ as well as the formation of SEI. And the peaks at 0.01~0.5 V are ascribed to the alloying reaction between Sn and Na^+ to form Na_xSn alloy. In the anodic sweep, the peaks at 0.09, 0.24 and 1.2 V correspond to the dealloying of Na_xSn alloy and conversion of Sn with Na_2S. And the peaks at 2.0 and 2.35 V are ascribed to the conversion of Na_2S to polysulfides.